PERGAMON

Vision Research 40 (2000) 2277–2289

Vision Research

www.elsevier.com/locate/visres

Exploring the dynamics of light adaptation: the effects of varying the flickering background's duration in the probed-sinewave paradigm

S. Sabina Wolfson *, Norma Graham

Department of Psychology, Columbia University, Mail Code 5501, New York, NY 10027, USA

Received 9 September 1999; received in revised form 22 February 2000

Abstract

In the probed-sinewave paradigm, threshold for detecting a probe is measured at various phases with respect to a sinusoidally-flickering background. Here we vary the duration of the flickering background before (and after) the test probe is presented. The adaptation is rapid; after approximately 10–30 ms of the flickering background, probe threshold is the same as that on a continually-flickering background. It is interesting that this result holds at both low (1.2 Hz) and middle (9.4 Hz) frequencies because at middle frequencies (but not at low) there is a *dc-shift*, i.e. probe threshold is elevated at all phases relative to that on a steady background (of the same mean luminance). We compare our results to predictions from Wilson's model [Wilson (1997), *Visual Neuroscience*, *14*, 403–423; Hood & Graham (1998), *Visual Neuroscience*, *15*, 957–967] of light adaptation. The model predicts the rapid adaptation, and the dc-shift, but not the detailed shape of the probe-threshold-versus-phase curve at middle frequencies.

Keywords: Light adaptation; Dynamics; Temporal frequency; Flicker; Computational model; Probed-sinewave paradigm

1. Introduction

As the ambient light level changes, the visual system must adapt in order to maintain sensitivity, since the response range of individual neurons is limited. Our overall goal is to develop a model of light adaptation. In this paper we examine the dynamics of rapid, moderate changes in light level using the probed-sinewave paradigm, and consider how well Wilson's (1997) model of light adaptation can account for our results.

The probed-sinewave paradigm is employed here since it has been shown to be a powerful tool in testing various models of light adaptation (Hood, Graham, von Wiegand & Chase, 1997). In a probed-sinewave task, the threshold for detecting a test probe is measured at various times on a flickering background. This type of experiment was introduced by Boynton, Sturr and Ikeda (1961), though they actually used square-wave modulation. Subsequent early work was done by Shickman (1970), and Maruyama and Takahashi (1977).

The probed-sinewave paradigm combines attributes of two other paradigms which have been used to study light adaptation. (i) A paradigm from the *periodic* tradition: temporal contrast sensitivity for a flickering light (e.g. de Lange, 1958; Kelly, 1961). (ii) A paradigm from the *aperiodic* tradition: the probe-flash technique in which threshold is measured for a small (spatially), brief (temporally) probe, presented on a larger, longer flash and/or steady background of light (e.g. Crawford, 1947; Battersby & Wagman, 1962; Geisler, 1978; Hood, 1978; Adelson, 1982). For excellent reviews of the light-adaptation literature see Shapley and Enroth-Cugell (1984), Hood and Finkelstein (1986) and Hood (1998).

The utility of the probed-sinewave paradigm can be seen in the context of a brief history of models of light adaptation. There have long been models to account for (aspects of) performance using the periodic and aperiodic stimuli mentioned above; but models which could account for phenomena from the periodic stimu-

* Corresponding author. Tel.: +1-212-8543006; fax: +1-212-8543609.

E-mail address: sabina@psych.columbia.edu (S.S. Wolfson).

0042-6989/00/$ - see front matter
PII: S0042-6989(00)00088-2

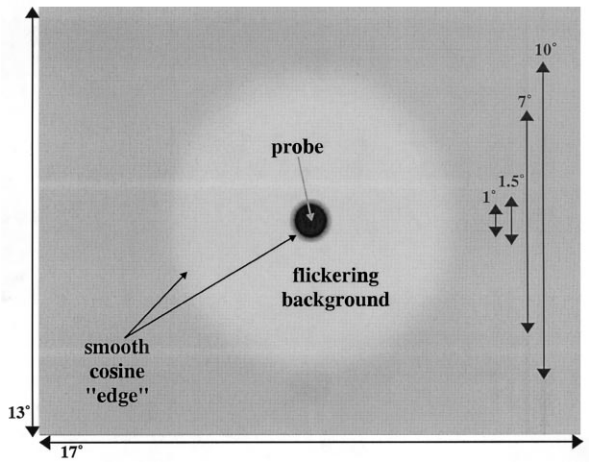

Fig. 1. Stimulus spatial configuration. The probe (with its smooth edge) subtends 1.5° of visual angle, and the flickering background (with its smooth edge) subtends 10° of visual angle. The probe is always a decrement in intensity with respect to the flickering background. The probe has been exaggerated in contrast for clarity; the flickering background in this example is at 45°.

lus tradition could not account for phenomena from the aperiodic stimulus tradition, and vice versa (Graham & Hood, 1992). Graham and Hood (1992) found that by combining certain key components of the periodic tradition models and the aperiodic tradition models, they could construct a *merged model* which could account for the different traditions' phenomena. However, when this merged model was tested with probed-sinewave data, it failed to account for key elements of that data (Hood et al., 1997). Subsequently, Hood and Graham (1998) tested Wilson's (1997) model of light adaptation using probed-sinewave data, and the model was found to account for much of the data. Thus, here we manipulate the probed-sinewave task to better understand the dynamics of light adaptation and to see if Wilson's model can account for these dynamics.

In the probed-sinewave experiments reported here, the test probe is a smooth-edged circle positioned in the center of a smooth-edged background as shown in Fig. 1. Temporally, the background flickers sinusoidally at some frequency, and (on a given trial) the test probe is shown at some phase with respect to the flickering background. In our stimuli, the probe is shown at one of eight possible phases with respect to the flickering background as indicated in the upper left panel of Fig. 2 (for the moment, ignore the lower panels). Typical results for 1.2 and 9.4 Hz flickering backgrounds are shown in Fig. 3. Threshold for detecting the probe is plotted as a function of the phase at which the probe was presented. We refer to these functions as *probe-threshold-versus-phase* curves. The three lower lines show results from three subjects with the 1.2 Hz flickering background, and the three higher lines show results from three subjects with the 9.4 Hz flickering background. Probe threshold on a steady background at the mean intensity of the flicker is shown by the dotted horizontal line plotted at 0.

What do these probe-threshold-versus-phase curves imply? If the visual system could 'immediately' adapt to any given light level, measuring probe threshold at some phase of a flickering background would be equivalent to measuring probe threshold on a steady back-

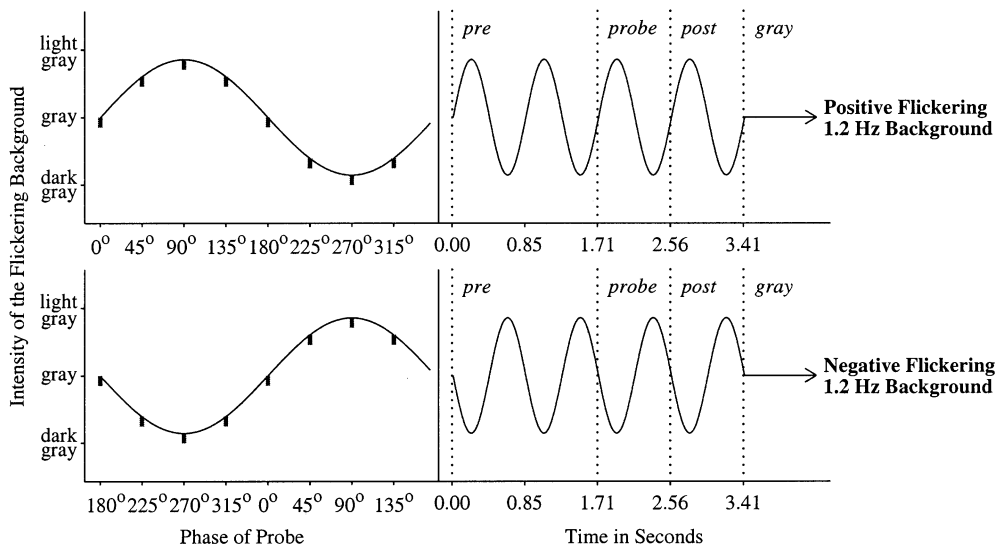

Fig. 2. Temporal details of experiments. The left panels show the eight different probe phases with respect to a positive flickering background (upper panel) and a negative flickering background (lower panel). On any given trial, the probe is presented at one of the eight phases, chosen at random. The right panels depict the time course of a trial in the continuous flicker condition for a positive flickering background (upper panel) and a negative flickering background (lower panel) at 1.2 Hz. Each trial has four events, which, in the continuous flicker condition, are: (i) approximately 2 s of flicker, followed by (ii) 1 cycle in which the probe is presented, followed by (iii) approximately 1 s of flicker, followed by (iv) at least 1 s of gray until the subject responds.

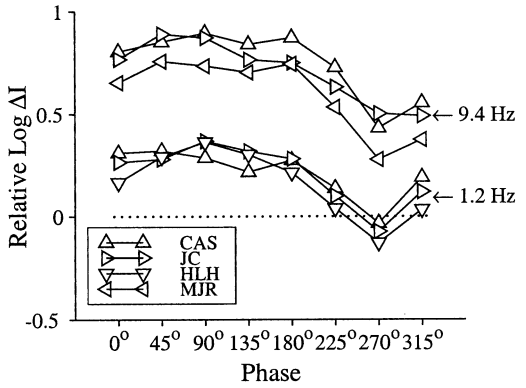

Fig. 3. Probe-threshold-versus-phase curves with 1.2 and 9.4 Hz (positive, continuous) flickering backgrounds. The upper three curves are the 9.4 Hz results, and the lower three curves are the 1.2 Hz results. The dotted line shows the threshold of the probe presented on a steady background at a luminance equal to the mean of the flickering background (steady-state probe threshold level). All subjects perform similarly. Notice that probe threshold is a function of phase: it is fairly constant between 0 and 180° and then drops at 270° (which is when the flickering background is dimmest).

ground with the same intensity. This is not the case (as shown in Fig. 3). On the other hand, if the visual system were very slow (averaging over the flickering background), phase should not matter. However, as shown in Fig. 3, threshold does vary as a function of phase. Further, probe thresholds with the 9.4 Hz flickering background are all elevated relative to probe thresholds with the 1.2 Hz flickering background. Stated another way, the 9.4 Hz probe-threshold-versus-phase curves have a higher *dc-level* than do the 1.2 Hz curves. A frequency-dependent dc-shift is a robust finding (e.g. Shickman, 1970; Hood et al., 1997; Wu, Burns, Elsner, Eskew & He, 1997; Shady, Chan & Hood, 1999).

Is there a slow process underlying the elevated dc-level at 9.4 Hz (where by 'slow' we mean at least a cycle or two)? Since the dc-level depends on frequency, one might think that it would take a cycle or two to develop. In the experiments reported here we vary the amount of flicker before (and after) the cycle of flicker in which the probe is presented. As we will show, the process underlying the dc-elevation turns out to be surprisingly fast ($\approx$10–30 ms) and, further, Wilson's (1997) model of light adaptation adequately predicts this rapid adaptation.

2. Methods

2.1. Subjects

The four subjects in this study were Columbia University undergraduates (or recent graduates) and were paid for their time. Subjects were naive as to the purpose of the experiments, but CAS, JC, and, MJR had experience in other probed-sinewave experiments. All subjects had a corrected visual acuity of 20/20 or better.

2.2. Stimuli and apparatus

The spatial configuration of an exemplar stimulus is shown in Fig. 1. The probe subtends 1.5° of visual angle, and the flickering background subtends 10° of visual angle at the viewing distance of 1 m. The probe is centered within the flickering background, and the flickering background is centered within the monitor's screen. Both the probe and flickering background have smooth cosine edges (radii of 0.25° and 1.5° of visual angle, respectively). Four sticks were attached to the edges of the monitor so that subjects could maintain fixation; the sticks extended 3° into the monitor, pointing towards the center of the screen. The modulation contrast of the flickering background was 57%.

The probe was always a decrement in intensity with respect to the flickering background. The probe was presented for one frame, and since the monitor presented 75 frames/s, the duration of one frame was approximately 13 ms. Due to phosphor decay, the probe was 'on' for a short part of this 13 ms, and then was 'off' (decayed) for the rest of the 13 ms. The mean intensity during this 13 ms interval is what we report as the probe's intensity.

Stimuli were presented on an AppleVision 1710 monitor controlled by an Apple Macintosh 9500. The mean luminance of the monitor was approximately 52 cd/m^2. The area of the screen beyond the flickering background was held steady at this mean luminance. Stimuli were generated and presented using MathWorks' MATLAB software in conjunction with the Psychophysics Toolbox (Brainard, 1997) and Video Toolbox (Pelli, 1997). Lookup-table values were set so that the relationship between pixel value and display luminance was linear. Subjects ran in a dimly lit room with free viewing.

2.3. Procedure and design

At the end of each trial the computer beeped, and the subject indicated whether they saw or did not see the probe by hitting the 'y' or 'n' key on the keyboard. After the subject responded, the computer beeped again to indicate that the next trial was beginning.

The intensity of the probe to be shown on each trial was determined by a QUEST (Watson & Pelli, 1983) staircase (60% threshold). In any given data-collecting session there were eight interleaved staircases (one staircase for each of the eight probe phases). Each staircase was 30 trials in length, resulting in 240 trials per session. Each session was repeated three times. Thus,

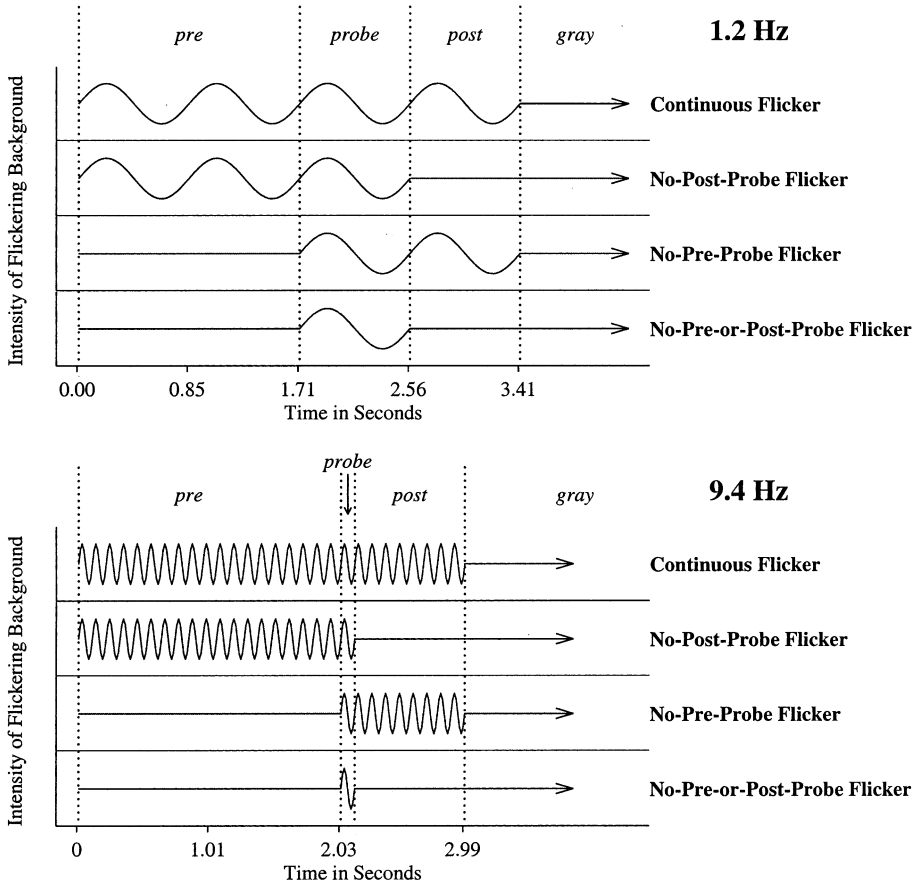

Fig. 4. Temporal details of the four different experimental time courses. A trial with any of the time courses consists of four events: (i) an approximately 2 s pre-event, (ii) a 1 cycle probe-event, (iii) an approximately 1 s post-event, and (iv) a gray-event of at least 1 s. During each event the background is either flickering (depicted as a sinewave), or continuous gray (depicted as a flat line). Note that the temporal profiles shown here are for positive flickering backgrounds; however, negative flickering backgrounds were also used.

each point in the data figures is the mean of three threshold estimates derived from 90 total trials (except for subject CAS's 1.2 Hz data which has only one or two threshold estimates in some cases). For each data collecting session there was a steady-state control session consisting of 30 trials. In the steady-state control session the background was continuous gray (at the same mean luminance as the flickering background). The steady-state control session was run directly before or after (randomly chosen) the data-collecting session.

There are 16 different data-collecting conditions which are described in Figs. 2 and 4 and in the text below. The 16 conditions are the combinations of

(two background waveform polarities)

$\times$ (four time courses) $\times$ (two frequencies)

The waveform polarities are termed *positive flickering background* and *negative flickering background* as shown in the upper and lower panels of Fig. 2, respectively. The four time courses are *continuous flicker*, *no-post-probe flicker*, *no-pre-probe flicker*, and *no-pre-or-post-probe flicker* as shown in Fig. 4. The two frequencies are 1.2 and 9.4 Hz, also shown in Fig. 4.

The left panels of Fig. 2 show the eight phases at which the decrement probe was presented on top of the sinusoidally-flickering background. The top panels show the positive flickering background and the bottom panels show the negative flickering background condition. The right panels each show the time course of one trial for the continuous flicker condition. A trial can be broken into four temporal events: *pre-event*, *probe-event*, *post-event*, and *gray-event*. For the continuous flicker condition they are: (i) approximately[1] 2 s of flickering background (*pre-event*), (ii) 1 cycle of flickering in which the probe is presented at a random phase (*probe-event*), (iii) approximately 1 s of flickering background (*post-event*), and (iv) a gray screen of at least 1 s until the subject responds (*gray-event*).

[1] The pre-event and post-event are *approximately* 2 and 1 s long (respectively) since we only used complete cycles of flicker. In terms of cycles, the pre-event is 2 cycles long (1.71 s) with the 1.2 Hz background, and 19 cycles long (2.03 s) with the 9.4 Hz background. Similarly, in terms of cycles, the post-event is 1 cycle long (0.85 s) with the 1.2 Hz background, and 8 cycles long (0.85 s) with the 9.4 Hz background. These 'odd' numbers are due to the monitors refresh rate (75 Hz).

The four different time course conditions (with a positive flickering background) are depicted in Fig. 4 for the 1.2 Hz flickering background (upper panel) and the 9.4 Hz flickering background (lower panel). The continuous flicker time course condition has the background flickering continuously during the pre-event, probe-event, and post-event.[2] The no-post-probe flicker time course condition has no flicker during the post-event. The no-pre-probe flicker time course condition has no flickering during the pre-event. The no-pre-or-post-probe flicker time course condition has no flickering during the pre-event or post-event. The gray-event is the same in all conditions.

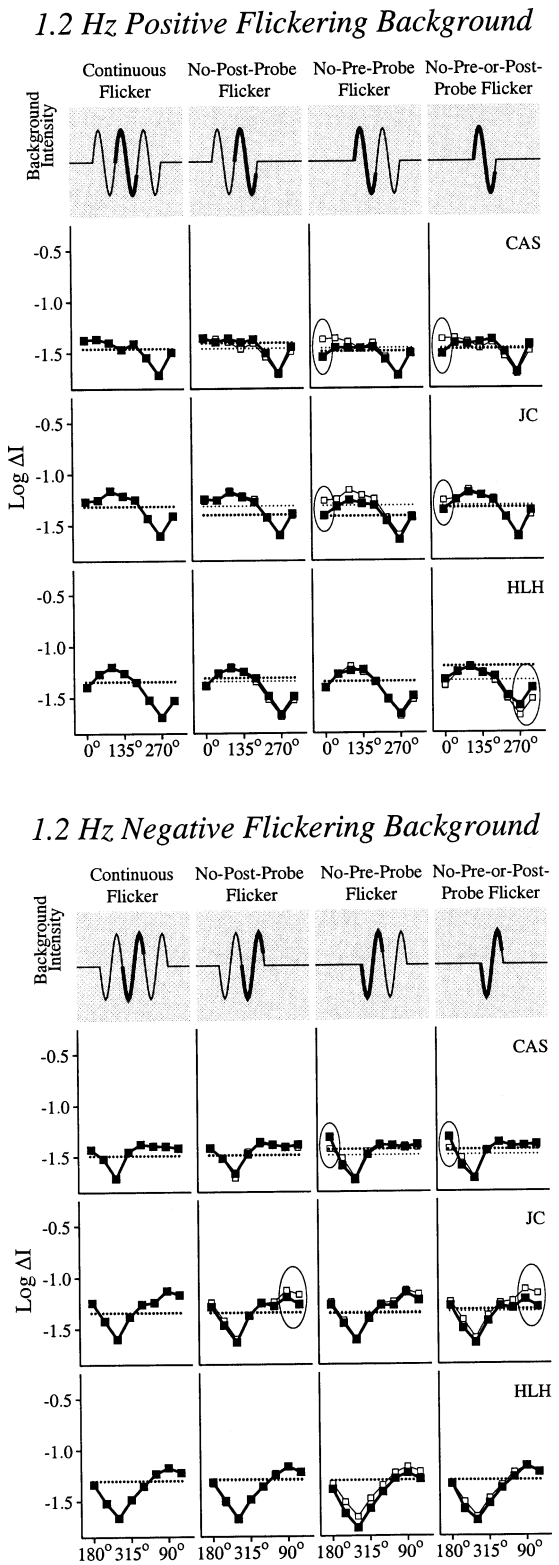

Fig. 5.

3. Experimental results

The results[3] are shown in Figs. 5 and 6 for the 1.2 and 9.4 Hz experiments, respectively. At the top of each column is an icon (on a light gray background) representing the experimental condition. The icon depicts whether the background flickered before and/or after the cycle in which the probe was presented; the probe cycle is highlighted by a bold line style. The upper panel of each figure contains the data obtained with a positive flickering background, and the lower panel contains the data obtained with a negative flickering background.

Each row of data in Figs. 5 and 6 shows the results from a subject (initials shown at far right) for the four time courses. The *closed* squares connected by bold lines show the subject's data in the condition depicted by the column's icon. The *open* squares connected by light lines are copies of the data from the far left column (the continuous flicker condition) for comparison purposes. The small circles show differences between the closed and open square curves which will be discussed below. The dotted horizontal lines are the

[2] Although there is no flickering between trials in our experiments, the results for our 'continuously flickering' condition are equivalent to results collected with a background that truly flickered continually (unpublished results).

[3] Error bars are not shown on the individual subject's graphs since they would be, nearly always, hidden by the symbols. The average (across subjects and conditions) SEM is 0.022 (the media is 0.020) log units. Error bars are shown on the larger summary plots in Figure 7 (which shows the mean of the subjects and ± 1 SE of that mean).

Fig. 5. Probe-threshold-versus-phase curves with a 1.2 Hz flickering background for three subjects. The upper half shows results with a positive flickering background; the lower half shows results with a negative flickering background. Each row contains results for a subject in all four conditions. At the top of each column is an icon depicting the experimental condition; data for that column's condition are shown with closed squares (and the associated steady-state level is the dark dotted line). The data from the far left column (continuous flicker) are shown as open squares in the other columns (and the associated steady-state level is the light dotted line). Small circles drawn around sections of the curves indicate phases at which the open and closed squares curves differ.

steady-state controls for the closed square data (dark dotted line) and for the open square data (light dotted line).

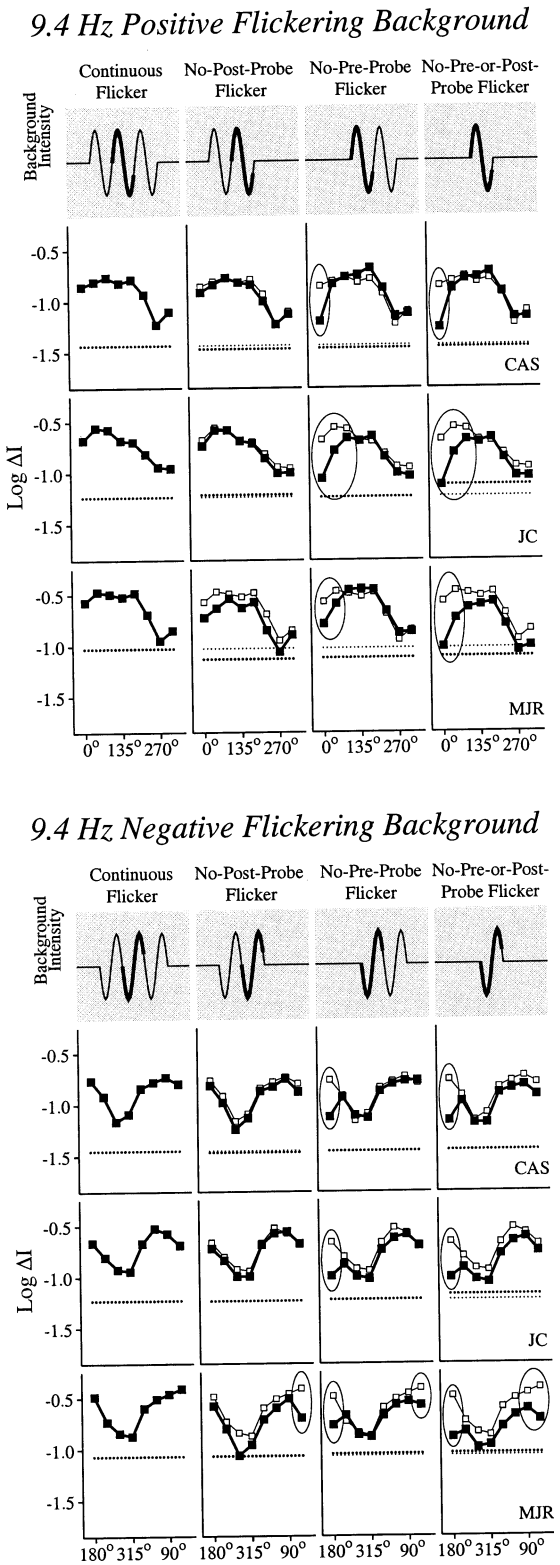

Fig. 6. Probe-threshold-versus-phase curves with a 9.4 Hz flickering background for three subjects. Same format as Fig. 5.

Before proceeding to the main results, notice that the shape of the probe-threshold-versus-phase curves with the positive flickering background (Figs. 5 and 6, top half) are generally consistent with the shape of the probe-threshold-versus-phase curves with the negative flickering background (Figs. 5 and 6, bottom half). In particular, if the negative flickering background results from the continuous flickering condition (far left column) are shifted over by 180° (half a cycle), the probe thresholds resemble those for the positive flickering background. Comparing the positive flickering background results with the negative flickering background results shows that the shape of the probe-threshold-versus-phase curves is not a function of time per se (first half versus last half of the cycle), but rather, a function of the direction in which the intensity of the background is varying (rising or falling half of the cycle).

3.1. Timing

Comparing the no-post-probe flicker condition to the continuous flicker condition (Figs. 5 and 6, second column from the left, closed versus open square results) shows little if any difference for both the 1.2 and 9.4 Hz results. Similarly, comparing the no-pre-or-post-probe flicker condition to the no-pre-probe flicker condition (Figs. 5 and 6, the closed squares in the fourth column versus the closed squares in the third column) shows little if any difference for both frequencies. There are a few cases where it appears that post-probe flicker may have an effect.[4] However, the inconsistency of this effect over subjects and conditions convinces us that it is not real. In summary, a background flickering *after* the probe cycle has little, if any, effect on probe threshold.

However, a background flickering *before* the probe cycle does make a small but systematic difference at the beginning of the probe-threshold-versus-phase curve. Comparing the no-pre-probe flicker condition to the

[4] Consider the circled data points at the ends of the probe-threshold-versus-phase curves in Figs. 5 and 6. For the 1.2 Hz positive flickering background (Fig. 5, upper panel), subject HLH shows a difference in the no-pre-or-post-probe flicker condition, but she does not show a difference in the no-post-probe flicker condition, suggesting that this is not a stable difference. For the 1.2 Hz negative flickering background (Fig. 5, lower panel), subject JC shows a difference in both the no-post-probe flicker condition and the no-pre-or-post-probe flicker condition, however, she does not replicate this result at 9.4 Hz (Fig. 6) or at 1.2 Hz with the positive flickering background. For the 9.4 Hz flickering background, the only subject who shows an effect of post-probe flicker is MJR with the negative flickering background (Fig. 6, lower panel). She shows a difference at the end of the probe-threshold-versus-phase curves for all the comparison conditions, suggesting that the difference is probably a function of probe threshold begin overly elevated in the continuous flicker condition.

continuous flicker condition (Figs. 5 and 6, third column from the left, closed versus open square results) shows many cases where probe thresholds in the continuous flicker condition are elevated relative to probe thresholds in the no-pre-probe flicker condition, though only at the start of the probe-threshold-versus-phase curves. The differences tend to be greater for the higher frequency (Fig. 6) than for the lower frequency (Fig. 5) and tend to be greater for the positive flickering background (Figs. 5 and 6 upper half) than for the negative flickering background (Figs. 5 and 6, lower half).[5] Similarly, comparing the no-pre-or-post-probe flicker condition to the no-post-probe flicker condition (Figs. 5 and 6, the closed squares in the fourth column to the closed squares in the second column) replicates this pattern of results. And, the direct comparison of the no-pre-or-post-probe flicker condition to the continuous flicker condition (Figs. 5 and 6, far right column, closed versus open square results) is also consistent.

Several panels in the 9.4 Hz results (Fig. 6) show slight vertical shifts with the open square (continuous flicker) above the closed squares. This is especially true for subject MJR. There is some possibility that this represents a true adaptation effect, with continuous flicker elevating the dc-level more. However, given the inconsistency of this effect, we think it more likely a criterion shift across conditions.

Thus, there are two main conclusions: (i) flickering *after* the probe cycle makes little difference; but (ii) flickering *before* the probe cycle produces elevated probe threshold at the beginning of the probe-threshold-versus-phase curve. There are also two subsidiary conclusions: (iii) the effects are more pronounced at the higher frequency than at the lower frequency; and (iv) the effects are generally more pronounced for the positive than for the negative flickering background. That the effects are more pronounced at the higher frequency than at the lower frequency (iii above) suggests that the duration of probe threshold elevation due to the pre-probe flicker is more a matter of *seconds* than of *cycles* (see next paragraph for details). If the effects are more pronounced for the positive-flickering than for the negative-flickering condition (iv above), this would mean that measuring probe threshold on the downswing of the background's cycle shows quicker adaptation. However, this result is not robust in our data and might be confounded by the fact that our probe is a decrement so we will say no more about it.

We estimate that the mechanisms underlying probe threshold take approximately 10–30 ms to adapt to a flickering background. We arrive at this estimate through the following logic. The 1.2 Hz results (Fig. 5) show that it takes at most 1/8th of a cycle (one phase) for probe threshold in the no-pre-probe flicker conditions to elevate to the level of probe threshold in the conditions with pre-probe flicker. Thus, in terms of seconds rather than cycles, this takes between 0 and 106 ms. The 9.4 Hz results (Fig. 6) give us a more refined estimate which is in agreement with the 1.2 Hz results. At 9.4 Hz it takes 1/8th–1/4th of a cycle[6] which translates to between 13 and 27 ms. Thus, we arrive at our (rounded) estimate of 10–30 ms.

3.2. dc-Level

The probe thresholds on the 1.2 Hz flickering background (Fig. 5, closed squares) are always within 0.5 log unit of the steady-state level (Fig. 5, dark dotted line). The probe threshold for the probe presented at 270° (valley of the sinewave) is actually below the steady-state level. Probe thresholds in the 9.4 Hz conditions (Fig. 6, closed squares) are more elevated than in the 1.2 Hz conditions, with all the probe thresholds being well above the steady-state level (Fig. 6, dark dotted line). This frequency-dependent dc-shift is like that reported by others (Shickman, 1970; Hood et al., 1997; Shady et al., 1999).

3.3. Curve shape

At 1.2 Hz (Fig. 5, left column), the shape of the probe-threshold-versus-phase curve is consistent with past results (e.g. Hood et al., 1997; Shady et al., 1999). At 9.4 Hz in our results (Fig. 6, left column), the shape is similar to that at 1.2 Hz except for the dc-level (as in the results of Shickman, 1970; e.g. Fig. 2). The general shape of our 9.4 Hz probe-threshold-versus-phase curves are different than some past results at medium frequencies (Maruyama & Takahashi, 1977; Hood et al., 1997; Shady et al., 1999), which, however, were often different from each other. In general, there is a great deal of variation in mid-frequency results from different labs (see Section 5).

3.4. Summary

The main results are summarized in Fig. 7. The figure shows the mean of the three subjects' probe-threshold-versus-phase curves for the continuous flicker (open circles) and no-pre-or-post-probe flicker (closed circles) conditions with a positive flickering background at 1.2 Hz (left panel) and 9.4 Hz (right panel). Error bars

[5] Note that for subject CAS with the 1.2 Hz negative flickering background, the effect is actually flipped.

[6] Although for subject JC with the positive flickering background (Fig. 6, upper panel) we have circled the first three phases, the effect at the third phase is so small that it would seem misleading to include it in our estimated range. It is not replicated on the negative flickering background, nor for the other subjects.

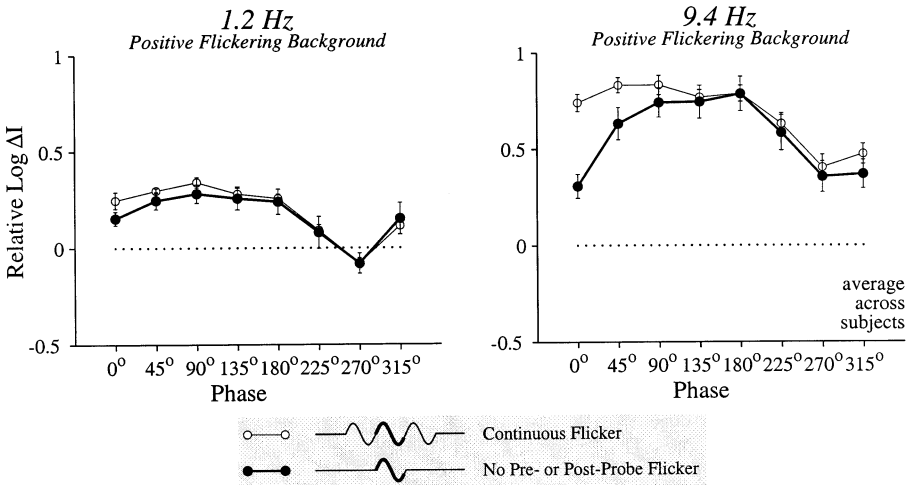

Fig. 7. Mean of the three subjects' probe-threshold-versus-phase curves at 1.2 Hz (left panel) and 9.4 Hz (right panel) with a positive flickering background. Two conditions are shown in each panel: the continuous flicker condition (open circles) and the no-pre-or-post-probe flicker condition (closed circles). Error bars show ± 1 SE of the mean.

show ± 1 SE of that mean. The main timing, dc-level, and curve shape effects discussed above can all be seen in this figure.

4. Modeling results

We have generated predictions using Wilson's (1997) model of light adaptation, which Hood and Graham (1998) found captured aspects of probed-sinewave data that previous models could not (Graham & Hood, 1992; Hood et al., 1997). Wilson's model is quite complex, and the interested reader should refer directly to it (Wilson, 1997). We will only describe the model very generally here since the aim of these particular simulations is quite modest: to see how well the model predicts our data using the same parameter settings as Hood and Graham (1998).

Wilson's (1997) model can be represented as a set of differential equations that describe the behavior of the various cell types found in the retina, followed by a very simplified 'visual cortex' (multi-stage low pass filter), followed by a simple decision rule (so that the model predictions can be compared to human psychophysical data). Within the model's retina there is one type of cone, one type of horizontal cell, four types of bipolar cells (On- and Off-center, M and P), two types of amacrine cells (On- and Off-center), one interplexiform cell, and four types of retinal ganglion cells (On- and Off-center, M and P).[7] A very important aspect of the connections between the cells is the push–pull process between the On- and Off-center bipolar cells. This push–pull process causes the cells that are responding more (either the On- or Off-center) to 'quiet' the other cells; the output from this process is then truncated at zero and used as input to the ganglion cells. The importance of this push–pull mechanism will be discussed below.

Our simulations are done in exactly the manner as those of Hood and Graham (1998). We (i) compute the output from the M–On and M–Off ganglion cells (the P cells are ignored since they are rather insensitive to our type of stimulus); (ii) use a peak–trough decision rule on the probe response within each pathway (M–On and M–Off); (iii) set the sensitivity of the Off pathway to be twice that of the On pathway; and (iv) assume the probe is detected by whichever pathway is most sensitive to it. The model parameters are the same as those used by Hood and Graham (1998), but the parameters describing the stimulus — i.e. the mean luminance, probe duration, and temporal profile of the stimulus — were changed to match those actually used in our experiments.

4.1. Timing

Wilson's (1997) model captures some of the temporal aspects of our data, as shown in Figs. 8 and 9 for 1.2 and 9.4 Hz, respectively. The model predictions in these figures are plotted using the same format as the psycho-

[7] The *cones* provide input to the horizontal and bipolar cells, and the cones receive subtractive feedback from the horizontal cells. The *horizontal* cells provide inhibitory input to the bipolar cells, and the horizontal cells receive feedback from amacrine cells via interplexiform cells. The *bipolar* cells provide input to ganglion cells (in separate M–On, M–Off, P–On, and P–Off pathways, where M and P refer to the type of ganglion cells to which the bipolar cells project) and amacrine cells (in separate On and Off pathways); bipolar cells also receive divisive feedback from the amacrine cells. Finally, the *ganglion* cells provide input to the 'visual cortex', and the ganglion cells receive inhibitory input from the amacrine cells.

physical data in Figs. 5 and 6; that is, for each condition (column) the model predictions are plotted with closed diamonds, and the models predictions from the continuous flicker condition (Figs. 8 and 9, far left column) have been copied over as the open diamonds onto all the other columns. The model makes the following predictions about the timing of adaptation and these predictions are in general agreement with our experimental results: (i) flickering the background *after* the probe cycle has little effect on probe threshold (Figs. 8 and 9, second column from left); (ii) flickering the background *before* the probe cycle elevates probe threshold at the beginning of the probe cycle (Figs. 8 and 9, third column from left); (iii) this elevation extends over more of the probe cycle with a 9.4 Hz flickering background than with a 1.2 Hz flickering background (compare Fig. 9 third column to Fig. 8 third column).

On the other hand, Wilson's (1997) model's predictions for the timing of adaptation do disagree with our results in several subtle ways, for example: (i) the effects

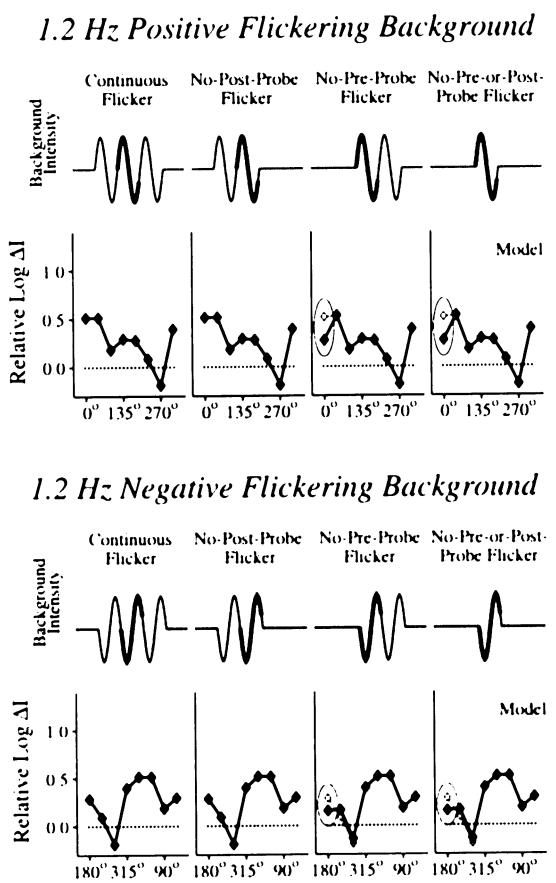

Fig. 8. Predictions from Wilson's model (Wilson, 1997; Hood & Graham, 1998). The model's predictions for the probe-threshold-versus-phase curves with a 1.2 Hz flickering background. These predictions are plotted in the same format as the psychophysical data in Fig. 5. The model captures the general temporal dynamics that were seen in the data.

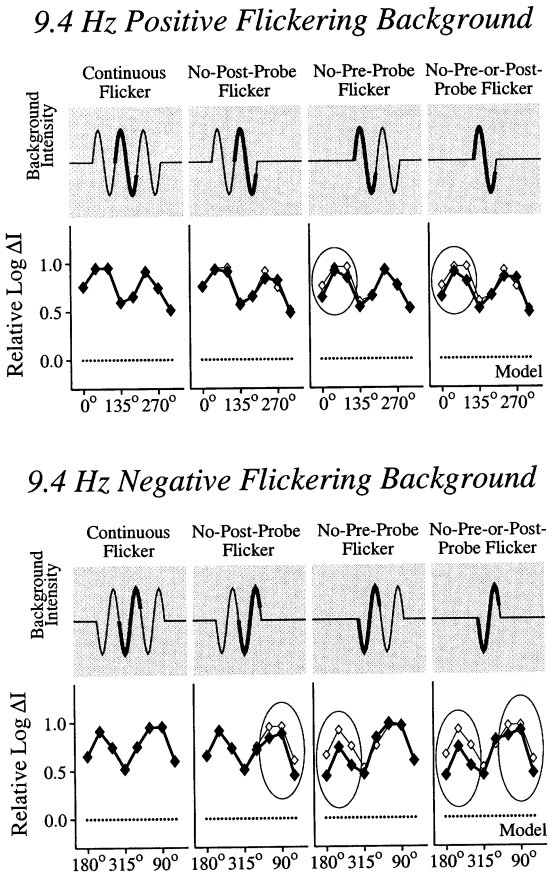

Fig. 9. Predictions from Wilson's model (Wilson, 1997; Hood & Graham, 1998). The model's predictions for the probe-threshold-versus-phase curves with a 9.4 Hz flickering background. These predictions are plotted in the same format as the psychophysical data in Fig. 5. The model captures the general temporal dynamics that were seen in the data.

of pre-probe flicker are not consistently greater for the positive flickering background than the negative flickering background (Figs. 8 and 9, upper row versus lower row); (ii) the model predicts that the effect of pre-probe flicker is larger (in magnitude) in the 1.2 Hz positive flickering background condition than in the 9.4 Hz positive flickering background condition (compare the difference between the open and closed diamonds in the right-hand columns, top row of Fig. 8 with the plots in the same positions in Fig. 9); (iii) post-probe flicker is predicted by the model to change probe threshold during the last half of the probe cycle for 9.4 Hz in the negative flickering background condition (Fig. 9, second and fourth column from left, bottom row), but only one subject shows this (Fig. 6, second and fourth column from left, bottom half, subject MJR).

These subtle disagreements may be secondary to disagreements described below about the shape of the probe-threshold-versus-phase curves. All these subtle timing disagreements are in the 9.4 Hz condition, which is where the shape prediction is problematic and where

different investigators' studies have produced different results. Any modification of the model that changed the overall shape of the probe-threshold-versus-phase curves might repair these subtle disagreements as well.

4.2. dc-Level

The thick gray lines in the upper panel of Fig. 10 show predictions from Wilson's (1997) model for the (positive, continuous) 1.2 and 9.4 Hz flickering background conditions. The psychophysical results are shown by black lines with symbols (reproduced from Fig. 3, which are the same results as those in Figs. 5 and 6, top half, far left column). The steady-state level is indicated by the horizontal dotted line at a relative probe threshold of 0. Notice that the model accurately predicts the dc-level at both 1.2 and 9.4 Hz.

The key element in the model producing the dc-level is the push–pull mechanism. If the push–pull mechanism is removed, then the dc-level drops dramatically, as shown by Hood and Graham (1998). The lower panel of Fig. 10 shows the same psychophysical data as in the upper panel along with predictions from the model *without* the push–pull mechanism (thick dashed gray lines). As can be seen, without the push–pull mechanism, predicted probe thresholds drop to near the steady-state level, and the shapes of the probe-threshold-versus-phase curves change dramatically (and do not resemble the psychophysical data).[8]

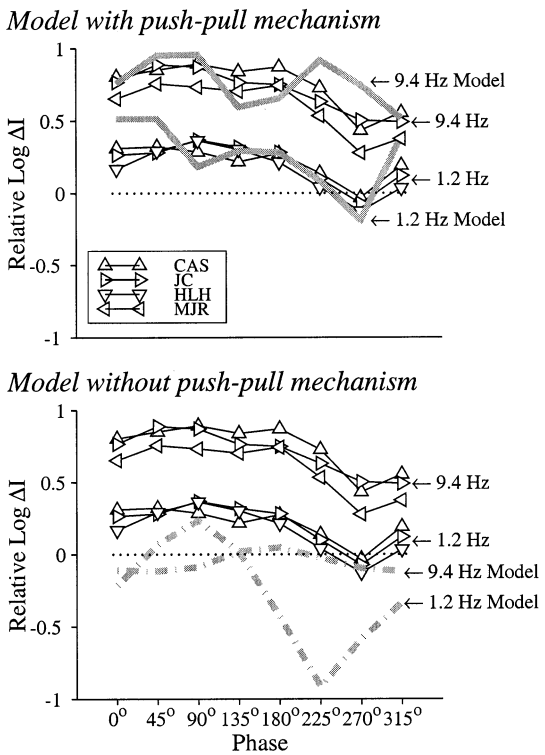

Fig. 10. Predictions from Wilson's model (Wilson, 1997; Hood & Graham, 1998) for the (positive, continuous) 1.2 and 9.4 Hz flickering backgrounds are shown as thick gray lines. Model predictions *with the push–pull* process are shown in the upper panel (thick, continuous, gray lines); model predictions *without the push–pull* process are shown in the lower panel (thick, dashed, gray lines). Psychophysical data are shown as symbols with thin black lines. With the push–pull mechanism in place, the model captures the dc-level at 1.2 and 9.4 Hz, and the shape of the probe-threshold-versus-phase curve at 1.2 Hz; however, the model does not capture the shape of the probe-threshold-versus-phase curve at 9.4 Hz. Without the push–pull mechanism in place, Wilson's model fails to account for all major aspects of the data.

4.3. Curve shape

The model captures rather well the shape of the 1.2 Hz probe-threshold-versus-phase curve (Fig. 10, upper panel) although it predicts a higher probe threshold near the positive zero-crossing (at phases 0, 45, 315°). The model fails to capture the details of the shape of the 9.4 Hz probe-threshold-versus-phase curve (Fig. 10, upper panel); the model predicts a curve with two peaks and a trough at approximately 135°, while the psychophysical data do not show a distinct peak and have a trough at 270°. The simplest way to summarize our 9.4 Hz data is to say that it resembles the 1.2 Hz data with a dc-shift. This is not true of the model's predictions.

4.4. Other models to consider

In Hood et al. (1997), five other models were considered. One, by Sperling and Sondhi (1968), was from the old periodic literature. Another one, MUSNOL, was from the old aperiodic literature based on work by Adelson (1982), Geisler (1978, 1979, 1981, 1983), Hood and colleagues (reviewed in Hood & Finkelstein, 1986; also Hayhoe, Benimoff & Hood, 1987), and Walraven and Valeton (1984). The other three models (Graham & Hood, 1992; von Wiegand, Hood & Graham, 1995) merged the key components of the older models. The two older models each accounted for results from its own tradition but failed to account for results from the other tradition (Graham & Hood, 1992). The three merged models could account for results from both traditions (Graham & Hood, 1992; von Wiegand et al., 1995) but, at least as originally investigated, fail to account for key features of the probed-sinewave paradigm results (Hood et al., 1997). However, as Wilson's (1997) model also fails to account for some aspects, it seems worthwhile to revisit these older models.

[8] *With* the push-pull mechanism in place, response levels are pulled down towards zero (recall that the push–pull output is truncated at zero). *Without* the push-pull mechanism, response levels are higher and do not get truncated. This appears to be very important in understanding the dc-elevation seen in the model with the push–pull mechanism in place since one can replace the push–pull mechanism with a constant subtraction and achieve some dc-elevation.

Our simulations with the five older models for the current experiments found four of the models to be entirely unsatisfactory. Sperling and Sondhi's (1968) model predicts no difference between any of the timing conditions. Three others (MUSNOL, and two of the merged models) sometimes predict a difference between the timing conditions but usually in the wrong direction, especially at 9.4 Hz. The remaining model (*Merged 2* in Graham & Hood, 1992) is not satisfactory but has more potential than we originally thought. On the positive flickering background, Merged 2 does as well as Wilson's (1997) model at predicting the timing effects. On the negative flickering background, however, Merged 2 predicts a difference for the later phases rather than the earlier.

Perhaps these older models, at least Merged 2, deserve some further attention. Some other newer models — such as those of Spitzer (Sherman & Spitzer, 1999; see also Dahari & Spitzer, 1996) and Shah and Levine (1996a,b) — may also be worth pursuing.

5. General discussion

Using the probed-sinewave experimental paradigm, we have examined the dynamics of light adaptation. After approximately 10–30 ms, probe threshold is elevated to the same level that it would have been had the background been continually flickering (Fig. 7 right panel, or Fig. 6 right-hand columns, compare open and closed symbols). Even at the very first phase with no preceding flickering, probe threshold is elevated relative to the steady-state control level (Fig. 7, compare far left closed symbols to the dashed line). Our results show that none of the probe threshold elevation — not even the dc-shift — is governed by a slow adaptation process.

Research using the probe-flash paradigm, coupled with careful modeling, also suggests very rapid adaptation processes (e.g. Hayhoe et al., 1987; Hayhoe, Levin & Koshel, 1992). They find that, following a small luminance step (0.5 log units) in the background, there is a rapid multiplicative process (complete within 50 ms) and a slower subtractive process (nearly complete within 200 ms, with substantial changes in the first 50 ms). The subtractive process takes much longer with a large luminance step (2.9 log units) in the background, taking 10–15 s to asymptote. Apparently this slower subtractive process does not show up in the probe-sine results here, perhaps because it is only substantial for larger luminance steps than we used.

Our results are consistent with some recent results from probed-sinewave experiments. Wu et al. (1997) examined the speed of light adaptation using a Gaussian windowed, 30 Hz sinusoidally flickering background on which a probe was presented. In one of their experiments, they placed a probe at each zero-crossing (i.e. all probes where shown at the mean intensity). They found that probe threshold elevation follows the Gaussian envelope, which is consistent with a fast growth of the dc-level, although other explanations are possible. Poot, Snippe and van Hateren (1999; see also Poot, Snippe & van Hateren, 1997) examined the dynamics of adaptation at the onset (and offset) of a 25 Hz flickering background. They started the flickering background at one of four different phases and averaged over these four backgrounds to estimate the dc-level in the probe-threshold-versus-phase curve. They found that, if the probe is delayed for approximately 40 ms, the estimated dc-level has asymptoted. This estimate is quite similar to ours in milliseconds although notice that, for their flickering rate, 40 ms is equivalent to a full cycle of flicker.

The shapes of the probe-threshold-versus-phase curves (with continuous flicker) measured here agree with some previous findings but disagree with others. In the 1.2 Hz flickering background condition (Fig. 5, far left column) the curves are very similar to those which have been previously reported (e.g. Hood et al., 1997; Shady et al., 1999). Our 9.4 Hz probe-threshold-versus-phase curves look very similar to the 1.2 Hz curves with a simple dc-shift (as do the results of Shickman, 1970; e.g. Fig. 2). But these results are unlike some previously reported results at similar frequencies (Maruyama & Takahashi, 1977; Hood et al., 1997; Shady et al., 1999). However, there is discrepancy regarding the shape of the probe-threshold-versus-phase curve at middle frequencies among these data sets. Interestingly, the dc-level is more stable across data sets.

Simulations with Wilson's (1997) model, using the same parameters as Hood and Graham (1998), show that the model can account for the dc-level at both 1.2 and 9.4 Hz (Fig. 10, upper panel: the psychophysical data shown with symbols are at the same height as the model's predictions shown with the thick gray lines). Further, the model accurately predicts the general shape of the 1.2 Hz probe-threshold-versus-phase curve. However, the model predicts a double-peak probe-threshold-versus-phase curve at 9.4 Hz which is quite different than the psychophysical data. Finally, the model, in general, agrees with the temporal aspects of the psychophysical data, showing that the continuous flicker probe thresholds are at the same level as the no-pre-probe flicker thresholds after 1/8th of a cycle with the 1.2 Hz flickering background (Figs. 5 and 8, right-hand columns, compare open and closed symbols) and after 3/8ths of a cycle with the 9.4 Hz flicker background (Figs. 6 and 9, right-hand columns, compare open and closed symbols).

In partial support of Wilson's (1997) model is recent work by Lee, Smith, Pokomy and Rüttiger (1999) who examined the responsivity of macaque ganglion cells to

a (high frequency) sinusoidally modulated probe on a (low frequency) sinusoidally modulated background. Their results with M ganglion cells look similar to the predictions of M ganglion cells shown by Hood and Graham (1998) for low frequency modulation. However, in other respects, the ganglion cell data of Lee et al. (1999) look quite different than those simulated by Wilson's model.

In summary, we find that adaptation to a flickering background is very quick, taking approximately 10–30 ms. This fast adaptation holds both for the dc-level in the probe-threshold-versus-phase curves and for the probe thresholds at individual phases. Wilson's model (Wilson, 1997; Hood & Graham, 1998) of light adaptation captures some aspects of the data, in particular, the fast timing and dc-level.

Acknowledgements

We would like to thank our subjects for their many hours of participation; Don Hood and Sherif Shady for helpful discussions; and Jenifar Chowdhury for her work on the data analyses and comments on this manuscript. Portions of this work were presented at the annual meeting of the Association for Research in Vision and Ophthalmology (Wolfson & Graham, 1999). The research was supported by National Eye Institute grant EY08459 to Norma Graham and EY06933 to Sabina Wolfson.

References

Adelson, E. H. (1982). Saturation and adaptation in the rod system. *Vision Research*, *22*, 1299–1312.

Battersby, W. S., & Wagman, I. H. (1962). Neural limitations of visual excitability. IV: spatial determinants of retrochiasmal interaction. *American Journal of Physiology*, *203*, 359–365.

Boynton, R. M., Sturr, J. F., & Ikeda, M. (1961). Study of flicker by increment threshold technique. *Journal of the Optical Society of America*, *51*, 196–201.

Brainard, D. H. (1997). The Psychophysics Toolbox. *Spatial Vision*, *10*, 443–446.

Crawford, B. H. (1947). Visual adaptation in relation to brief conditioning stimuli. *Proceedings of the Royal Society B*, *134*, 283–302.

Dahari, R, & Spitzer, H. (1996). Spatiotemporal adaptation model for retinal ganglion cells. *Journal of the Optical Society of America*, *13*, 419–435.

Geisler, W. S. (1978). Adaptation, afterimage and cone saturation. *Vision Research*, *18*, 279–289.

Geisler, W. S. (1979). Initial image and afterimage discrimination in the human rod and cone systems. *Journal of Physiology*, *294*, 165–179.

Geisler, W. S. (1981). Effects of bleaching and backgrounds on the flash response of the cone system. *Journal of Physiology*, *312*, 413–434.

Geisler, W. S. (1983). Mechanisms of visual sensitivity: backgrounds and early dark adaptation. *Vision Research*, *23*, 1423–1432.

Graham, N., & Hood, D. C. (1992). Modeling the dynamics of light adaptation: the merging of two traditions. *Vision Research*, *32*, 1373–1393.

Hayhoe, M. M., Benimoff, N. I., & Hood, D. C. (1987). The time-course of multiplicative and subtractive adaptation process. *Vision Research*, *27*, 1981–1996.

Hayhoe, M. M., Levin, M. E., & Koshel (1992). Subtractive processes in light adaptation. *Vision Research*, *32*, 323–333.

Hood, D. C. (1978). Psychophysical and electrophysiological tests of physiological proposals of light adaptation. In J. Armington, J. Krauskopf, & B. Wooten, *Visual psychophysics: its physiological basis* (pp. 141–155). New York: Academic Press.

Hood, D. C. (1998). Lower-level visual processing and models of light adaptation. *Annual Review of Psychology*, *49*, 503–535.

Hood, D. C., & Finkelstein, M. A. (1986). Sensitivity to light. In K. R. Boff, L Kaufman, & J. P. Thomas, *Visual psychophysics: its physiological basis*. New York: Academic Press.

Hood, D. C., & Graham, N. (1998). Threshold fluctuations on temporally modulated backgrounds: a possible physiological explanation based upon a recent computational model. *Visual Neuroscience*, *15*, 957–967.

Hood, D. C., Graham, N., von Wiegand, T. E., & Chase, V. M. (1997). Probed-sinewave paradigm: a test of models of light-adaptation dynamics. *Vision Research*, *37*, 1177–1191.

Kelly, D. H. (1961). Visual responses to time-dependent stimuli: II. Single channel model of the photopic visual system. *Journal of the Optical Society of America*, *51*, 747–754.

de Lange, H. (1958). Research into the dynamic nature of the human fovea-cortex systems with intermittent and modulated light. *Journal of the Optical Society of America A*, *7*, 2223–2237.

Lee, B. B., Smith, V. C., Pokomy, J., & Rüttiger, L. (1999). Macaque ganglion cell responsivity on sinusoidally modulated backgrounds. *Investigative Ophthalmology and Visual Science*, *40* (Suppl.), 4303 (Abstract).

Maruyama, K., & Takahashi, M. (1977). Wave form of flickering stimulus and visual masking function. *Tohoku Psychologica Folia*, *36*, 120–133.

Pelli, D. G. (1997). The VideoToolbox software for visual psychophysics: Transforming numbers into movies. *Spatial Vision*, *10*, 437–442.

Poot, L., Snippe, H. P., & van Hateren, J. H. (1997). Dynamics of adaptation at high luminances: Adaptation is faster after luminance decrements than after luminance increments. *Journal of the Optical Society of America A*, *14*, 2499–2508.

Poot, L., Snippe, H. P., & van Hateren, J. H. (1999). Dynamics of adaptation to the onset and offset of flicker. *Investigative Ophthalmology and Visual Science*, *40*, Abstract #249.

Shady, S., Chan, K., & Hood, D. C. (1999). The dynamics of light-adaptation of the rod and cone systems. *Investigative Ophthalmology and Visual Science*, *40* (Suppl.), 246 (Abstract).

Shah, S., & Levine, M. D. (1996a). Visual information processing in primate cone pathways-part I: a model. *IEEE Transactions on Systems, Man and Cybernetics, Part B: Cybernetics*, *26*, 259–273.

Shah, S., & Levine, M. D. (1996b). Visual information processing in primate cone pathways-part II: experiments. *IEEE Transactions on Systems, Man and Cybernetics, Part B: Cybernetics*, *26*, 255–289.

Shapley, R., & Enroth-Cugell, C. (1984). Visual adaptation and retinal gain controls. In N. N. Osborne, & G. J. Chader, *Progress in retinal research* (pp. 263–343). Oxford: Pergamon Press.

Sherman, E., & Spitzer, H. (1999). Adaptation mechanisms in the visual system to periodic stimulus. *Fifth IBRO World Congress of Neuroscience*, Jerusalem, Israel, 11–16 July 1999.

Shickman, G. M. (1970). Visual masking by low-frequency

sinusoidally modulated light. *Journal of the Optical Society of America*, *60*, 107–117.

Sperling, G., & Sondhi, M. M. (1968). model for visual luminance discrimination and flicker detection. *Journal of the Optical Society of America*, *58*, 1133–1145.

Walraven, J., & Valeton, J. M. (1984). Visual adaptation and response saturation. In A. J. Van Doorn, W. A. Van de Grind, & J. J. Koenderink, *Limits in perception* (pp. 401–429). Utrecht: VNU Science Press.

Watson, A. B., & Pelli, D. G. (1983). QUEST: a Bayesian adaptive psychometric method. *Perception and Psychophysics*, *33*, 113–120.

von Wiegand, T. E., Hood, D. C., & Graham, N. V. (1995). Testing a computational model of light-adaptation dynamics. *Vision Research*, *35*, 3037–3051.

Wilson, H. R. (1997). A neural model of foveal light adaptation and afterimage formation. *Visual Neuroscience*, *14*, 403–423.

Wolfson, S. S., & Graham, N. (1999). Rapid light adaptation: the effects of varying the background's duration in the probe-sinewave paradigm. *Investigative Ophthalmology and Visual Science*, *40* (Suppl.), 247 (Abstract).

Wu, S., Burns, S. A., Elsner, A. E., Eskew, R. T., & He, J. (1997). Rapid sensitivity changes on flickering backgrounds: tests of models of light adaptation. *Journal of the Optical Society of America A*, *14*, 2367–2378.